Neoplasia 62 (2025) 101144

Contents lists available at ScienceDirect

Neoplasia

journal homepage: www.elsevier.com/locate/neo

Original Research

m6A eraser ALKBH5/treRNA1/DDX46 axis regulates BCR expression

Bandish Kapadia [a,b,c,*], Anirban Roychowdhury [a,b,c], Forum Kayastha [a,b,c], Won Sok Lee [d], Nahid Nanaji [e], Jolene Windle [c,f,g], Ronald Gartenhaus [a,b,c,*]

[a] Division of Hematology, Oncology, and Palliative Care, Department of Internal Medicine, School of Medicine, Virginia Commonwealth University, Richmond, VA, USA
[b] Section of Hematology and Oncology, Medicine Service, Richmond VA Cancer Center, Richmond Veteran Affairs Medical Center, Richmond, VA, USA
[c] VCU Massey Comprehensive Cancer Center, Virginia Commonwealth University, School of Medicine, Richmond, VA 23298, USA
[d] Department of Pathology, Richmond Veteran Affairs Medical Center, Richmond, VA, USA
[e] Department of Veteran Affairs, Maryland Healthcare System, Baltimore, MD, USA
[f] Department of Human and Molecular Genetics, Virginia Commonwealth University, School of Medicine, Richmond, VA 23298, USA
[g] VCU Institute of Molecular Medicine, Virginia Commonwealth University, School of Medicine, Richmond, VA 23298, USA

ARTICLE INFO

Keywords:
Epitranscriptomics
N6-methyladenosine (m6A)
ALKBH5
RNA demethylation
treRNA1
DDX46
B-cell receptor signaling
Immune regulation
Oncogenic pathways

ABSTRACT

Epitranscriptomic modifications, particularly N6-methyladenosine (m6A), have emerged as critical regulators of RNA stability, localization, and translation, shaping immune responses and tumor progression. In B-cell biology, m6A modifications influence germinal center formation and antigen-driven differentiation, underscoring their importance in immune regulation. Among m6A regulators, ALKBH5 (RNA demethylase) is pivotal in removing methylation marks and modulating gene expression in diverse cellular contexts. Despite advancements in understanding m6A dynamics, the mechanistic interplay between m6A demethylation and B-cell receptor (BCR) signaling pathways still needs to be explored. This study reveals a novel regulatory axis involving ALKBH5, treRNA1 (Translation Regulatory Long Non-Coding RNA 1), and DDX46 (RNA helicase). Upon activation signals, ALKBH5 and treRNA1 translocate to the nucleus, forming a functional complex with DDX46 to orchestrate the removal of m6A modifications on key transcripts, including those involved in BCR signaling. This demethylation enhances transcript stability and facilitates cytoplasmic export through interaction with the RNA-binding protein HuR, promoting efficient translation. Disruption of this axis, via loss of ALKBH5, DDX46, or treRNA1, led to impaired transcript processing and diminished BCR-related gene expression, highlighting the critical role of m6A demethylation in maintaining RNA dynamics. These findings uncover a previously unrecognized epitranscriptomic mechanism driven by the ALKBH5-treRNA1-DDX46 complex, with significant implications for B-cell functionality, immune regulation, and oncogenic pathways. Targeting this axis offers a promising avenue for developing therapeutic strategies in cancer and immune-related disorders where m6A dysregulation plays a central role.

Introduction

B-cells are pivotal in adaptive immunity, safeguarding the host by recognizing pathogens and differentiating into plasma cells that secrete pathogen-specific antibodies. B-cell activation is initiated by antigen binding to the B-cell receptor (BCR), triggering cascades that drive proliferation and affinity maturation within germinal centers [1]. These signaling pathways define a mature lymphocyte's functionality and fate. However, aberrant activation of the BCR pathway is a hallmark of B-cell leukemias and lymphomas, fueling tumor proliferation and making it an attractive therapeutic target [2,3]. Over the past few decades, BCR-targeted therapies have emerged as promising alternatives to conventional chemoimmunotherapy, but their clinical application often falls short of producing durable responses [4,5]. Challenges include inherent biological complexity, resistance mechanisms, and significant toxicities when combined with standard regimens like R-CHOP. Emerging evidence suggests that epitranscriptomic modifications—chemical alterations of RNA without changing its sequence—may critically influence B cell activation by modulating transcript stability, translation efficiency, and interactions with regulatory proteins [6–8]. Indeed, emerging data highlight the underappreciated role of epitranscriptomic modifications in regulating B cell functionality,

* Corresponding authors.
E-mail addresses: bandish.kapadia@vcuhealth.org (B. Kapadia), Ronald.gartenhaus@vcuhealth.org (R. Gartenhaus).

https://doi.org/10.1016/j.neo.2025.101144
Received 8 January 2025; Received in revised form 10 February 2025; Accepted 18 February 2025
Available online 22 February 2025

potentially driving tumorigenesis and resistance to targeted therapies. These dynamic RNA modifications, such as N6-methyladenosine (m6A), have been implicated in both physiological B-cell processes and oncogenic pathways.

The proper function of B-cells in adaptive immunity depends on tightly regulated signaling cascades initiated by antigen binding to the B-cell receptor (BCR) [9]. This activation triggers BLK-mediated phosphorylation of CD79A (Ig-alpha) and CD79B (Ig-beta), subsequently activating downstream pathways, including BTK and CARD11, that drive NF-κB and MAPK signaling [10–12]. These pathways are critical for B-cell activation, proliferation, and survival. Given the central role of BCR signaling in maintaining B-cell homeostasis, its dysregulation is a key driver of B-cell malignancies, particularly Diffuse Large B-Cell Lymphoma (DLBCL)—the most common and aggressive form of non-Hodgkin lymphoma. DLBCL is characterized by significant molecular and clinical heterogeneity, with genetic alterations frequently leading to constitutive BCR activation, fueling tumor proliferation and survival [12–15]. Despite extensive characterization of downstream BCR signaling, upstream regulatory mechanisms, including post-transcriptional and translational controls, remain less explored. Our previous studies revealed that BCR mimetics enhance eIF4A-dependent [16] BCR signalosome expression, while HuR promotes BCR transcript translation [17]. However, the regulatory role of RNA modifications in shaping these processes is poorly understood. A deeper understanding of these regulatory layers could provide novel therapeutic opportunities in DLBCL.

The field of epitranscriptomics has transformed our understanding of gene regulation, particularly in immune and oncogenic contexts. N6-methyladenosine (m6A), the most prevalent RNA modification, dynamically regulates RNA stability, localization, and translation in processes essential to cellular homeostasis and tumorigenesis [18–21]. Mediated by m6A writers (e.g., METTL3, METTL14), erasers (e.g., ALKBH5), and readers (e.g., YTHDF2), this reversible modification integrates diverse signaling networks, including those underlying immune responses. In B-cell biology, m6A has been shown to influence pre-B cell transition [7,22] and germinal center development [8] by modulating key transcripts. Dysregulated m6A pathways, however, are often exploited in cancer, enabling malignant cells to adapt to stress, evade immune surveillance, and sustain oncogenic signaling. For instance, m6A-mediated regulation of CD40 signaling in B-cells highlights its potential role in immune-modulatory pathways [23]. Thus, dysregulated m6A contributes to immune evasion and resistance mechanisms commonly observed in B-cell lymphomas by altering the stability and translational output of key immune and oncogenic transcripts.

Materials and methods

Ethics declaration

All experiments were conducted according to relevant Institutional guidelines and regulations related to the Care and Use of Laboratory Animals. All animal procedures were approved by the Institutional Animal Care and Use Committee of Richmond VAMC and were per the 2011 Eighth Edition of the NIH Guide for the Care and Use of Laboratory Animals. Human tissue samples were acquired through the R. Adams Cowley Shock Trauma Center and University of Maryland Greenebaum Cancer Center Pathology Biorepository and Research Core. They were compliant with research ethics stated by the University of Maryland Medical School. All donors completed University of Maryland Institutional Review Board-approved consent documents. They were informed via these consent documents that the donated tissue would be used for distribution to qualified researchers and that such distributions could be made at any time. These consent documents also assured that the donor's identity would remain unknown to any tissue recipients and those reviewing the results of their work.

B-cell activation assay

Human B-cells (5×10^6) were cultured in 100 cm tissue culture dishes (BD Falcon). These culture dishes were pre-seeded overnight with B- cell culture media (RPMI 1640 with 10 % human serum (Sigma-Aldrich), 55 μM 2-mercaptoethanol, 2 mM l-glutamine, 100 U/ml penicillin, 100 μg/ml streptomycin, 10 mM HEPES, 1 mM sodium pyruvate and 1 % MEM nonessential amino acids) [24]. The following day, human B cells were exposed to treatment with mouse IgG1κ (isotype control; eBioscience), anti-human IgA+IgG+IgM(*H* + L) (anti-BCR; Jackson ImmunoResearch), anti-CD40 clone 5C3 (anti-CD40; eBioscience), or anti-BCR + anti-CD40 and maintained for 24 h [16]. Each B-cell culture reached a final 6 ml/dish volume when using 10 cm dishes.

Institutional review board statement

This study is reported under ARRIVE guidelines (https://arriveguidelines.org). Richmond VAMC approved the study, protocol # 1572637, 1676330, 1721572, and 1610627.

Mice and immunization

EμMyc$^{\pm}$ (B6.Cg-Tg(IghMyc)22Bri/J) and Wild type mice (C57Bl/6, Strain #:000664) were procured from The Jackson Laboratory. For breeding, EμMyc heterozygote males were mated with wild-type females. Once the mice developed spontaneous tumors, animals were humanely euthanized, and the tumor was preserved for immunohistochemistry and/or downstream molecular biology experiments. Wild-type mice were intraperitoneally injected with 100 μL of 20 % SRBC for immunization. Seven days post-injection, mice were humanely euthanized, and the spleen was collected for IHC or single-cell sorting. All mice were housed in a clean and antigen-free environment in the Transgenic/Knockout Mouse Shared Resource and/or at Richmond Veterans Affairs Medical Center (Richmond, VA). All mice were housed in groups of ≤5 mice/cage, maintained in a temperature- and humidity-controlled environment with a 12 h light-dark cycle, and provided with food and water ad libitum. Mice were age and sex-matched within each experiment (both males and females were used). All experimental procedures involving animals complied with the guidelines outlined by the animal component of the research protocol (ACORP) at the Richmond Veterans Affairs Medical Center and received proper approval.

Global m6A/m measurements

Quantification of m6A RNA methylation was detected by an m6A RNA methylation assay kit (Epigentek Group, Farmingdale, NY) following the manufacturer's protocol. Total RNA samples of 200 ng for each group were used to determine the percentage of m6A. The absorbance was measured at 450 nm using a microplate reader, and the percentage of m6A in total RNA was calculated using the following equation:

$$m6A\% = ((\text{Sample OD} - \text{Blank}) \div S) / ((\text{Positive Control OD} - \text{Blank}) \div P) \times 100\%$$

where S represents the amount of input RNA sample in ng, and P represents the amount of positive control input in ng.

ALKBH5 demethylase assay

The in vitro ALKBH5 demethylation activity assay was performed as previously reported with minor modifications [25,26]. Briefly, the reactions were performed in a 50 μl demethylation reaction buffer containing 2 μg of total RNA resuspend in 50 mM HEPES pH 7.5, 100 μM 2OG, 100 μM Ascorbate, 50 μM (NH4)2Fe(SO4)2·6H2O and 1 mM TCEP.

The reaction was incubated at room temperature for 2 h. Post-reaction was purified as described earlier for downstream analysis.

MeRIP and HuR IP-RT-qPCR

All the specific manipulations were performed according to the protocol of Magna MeRIP™ m6A Kit (Catalog No 17–10,499, Merck Millipore) with minor modifications. Briefly, total RNA was subjected to immunoprecipitation with antibody, and the elute RNA was subjected to cDNA synthesis as described earlier. For HuR RNA enrichment, recombinant HuR (N-terminal GST-tagged, Abcam, ab152360) was incubated with purified RNA (2 µg) in HuR-RIP buffer (150 mM KCl, 25 mM Tris-HCl pH 7.4, 5 mM EDTA, 0.5 mM dithiothreitol, 0.05 % NP-40, 100 µg/ml RNAse inhibitor RiboLock (Thermo Fisher Scientific, Waltham, MA, USA) for 4 h at 4°C on rotation. Prewashed GST Sepharose beads (40 µL) were added to each sample and rotated for 1 h. The beads were washed with HuR-RIP buffer, and RNA was isolated with a trizol reagent. Purified Luciferase mRNA (10 pg) was added to each cDNA synthesis reaction as the internal control.

Additional technical details are provided in supplemental Materials.

Results

RNA methylation dynamics are altered in normal and malignant B-cell SIGNALING

The regulation of gene expression in B-cells is intricately controlled at the transcriptional and translational levels and through post-

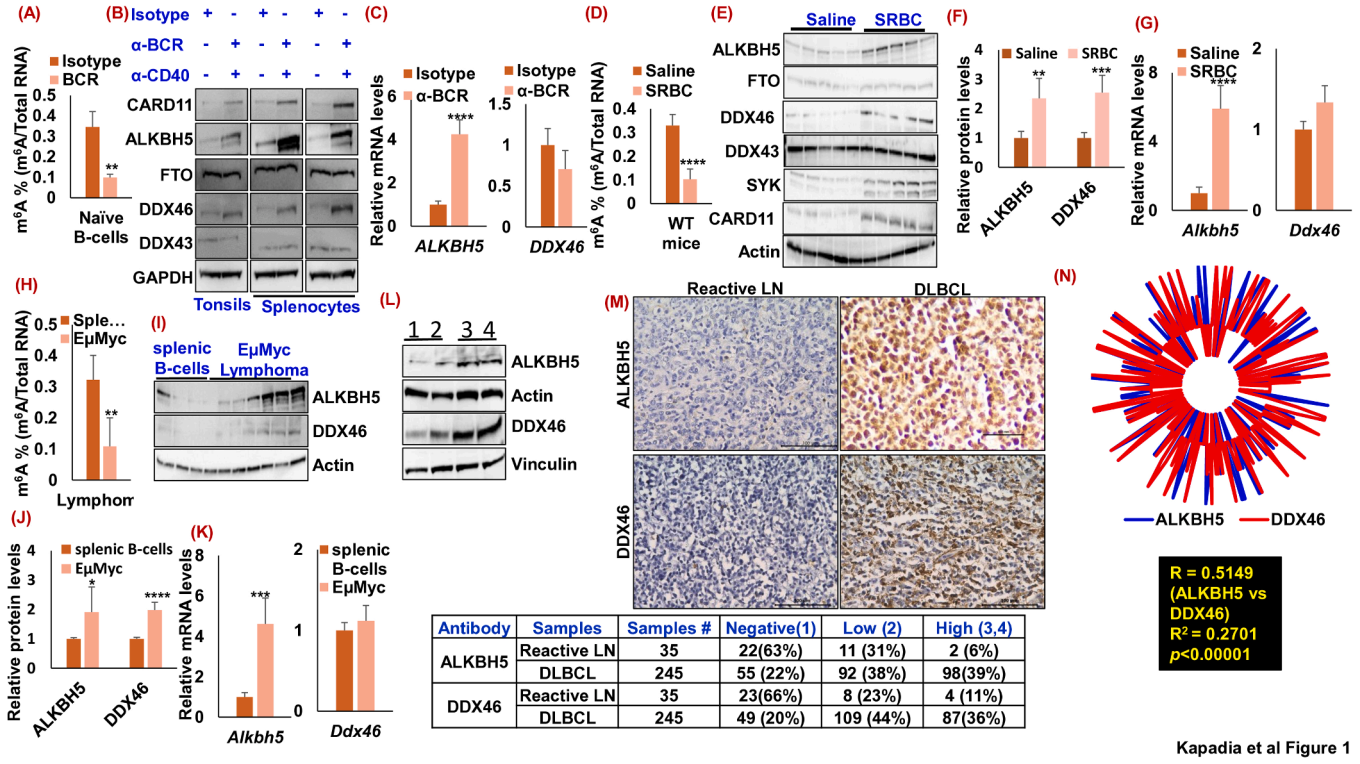

Antibody	Samples	Samples #	Negative(1)	Low (2)	High (3,4)
ALKBH5	Reactive LN	35	22(63%)	11 (31%)	2 (6%)
	DLBCL	245	55 (22%)	92 (38%)	98(39%)
DDX46	Reactive LN	35	23(66%)	8 (23%)	4 (11%)
	DLBCL	245	49 (20%)	109 (44%)	87(36%)

Kapadia et al Figure 1

Fig. 1. Induction of ALKBH5 and DDX46 Expression by BCR Mimetics Enhances RNA Demethylation: (A) Naïve B-cells were exposed to BCR mimetics or isotype antibodies, and total RNA was collected after 24 h for m6A quantification. The results were normalized with total RNA and expressed as mean±SD. Statistical analysis was performed using an unpaired, two-tailed Student's *t*-test. $^{**}p < 0.01$ vs. isotype-treated cells. (B) Protein lysates were harvested from the naïve B-cells after 24 h of treatment with BCR mimetics or isotype and were analyzed using immunoblotting with the indicated antibodies. (C). Total RNA was subjected to quantification of *ALKBH5* and *DDX46* with real-time quantitative PCR (RT-qPCR). The results were normalized with *GAPDH* (reference gene), set to 1 for Isotype treatment, and expressed as mean±SD. Statistical analysis was performed using an unpaired, two-tailed Student's *t*-test. $^{****}p < 0.001$ vs. Isotype-treated cells. (D) Wild-type mice were injected with SRBC or saline, and the total splenic B-cell RNA was isolated after 7 days of injection for m6A quantification. The results were normalized with total RNA and expressed as mean±SD. Statistical analysis was performed using an unpaired, two-tailed Student's *t*-test. $^{****}p < 0.001$ vs saline-treated cells. (E) Protein lysates were harvested from the splenic B-cells of wild-type mice after 7 days of injection with SRBC or saline and were analyzed using immunoblotting with the indicated antibodies. (F) Densitometric quantifications of immunoblots of ALKBH5 and DDX46 from Fig. 1E. Values were first normalized with their respective loading controls (Actin) and neutralized with the average of saline injected B cells and expressed as mean ± SD, which was set at 1. Statistical analysis was performed using an unpaired, two-tailed Student's *t*-test. $^{**}p < 0.01$ vs saline-treated cells. (G) Total RNA was subjected to quantification of *Alkbh5* and *Ddx46* with RT-qPCR. The results were normalized with *Gapdh* (reference gene), set to 1 for saline-injected cells, and expressed as mean±SD. Statistical analysis was performed using an unpaired, two-tailed Student's *t*-test. $^{****}p < 0.001$ vs saline injected cells. (H) EμMyc tumors and non-immunized splenic B-cells isolated RNA were subjected to m6A quantification. The results were normalized with total RNA and expressed as mean±SD. Statistical analysis was performed using an unpaired, two-tailed Student's *t*-test. $^{**}p < 0.01$ vs splenic non-immunized B-cells. (I) Protein lysates were harvested from EμMyc tumors and non-immunized splenic B-cells and were analyzed using immunoblotting ALKBH5 and DDX46. (J) Densitometric quantifications of immunoblots of indicated antibodies from Fig. 1I. Values were first normalized with their respective loading controls (Actin) and neutralized with the average of splenic non-immunized B-cells and expressed as mean ± SD, which was set at 1. Statistical analysis was performed using an unpaired, two-tailed Student's t-test. $^{*}p < 0.05$ vs splenic non-immunized B-cells. (K) Total RNA isolated from EμMyc and splenic non-immunized B-cells was subjected to quantification of *Alkbh5* and *Ddx46* with RT-qPCR. The results were normalized with *Gapdh* (reference gene), set to 1 for splenic non-immunized B-cells, and expressed as mean±SD. Statistical analysis was performed using an unpaired, two-tailed Student's *t*-test. $^{***}p < 0.005$ vs splenic non-immunized B-cells. (L) Protein lysates from naïve B-cells (splenic (1) and tonsils (2)) and primary DLBCL tumors (3 &4) were subjected to immunoblotting with indicated antibodies. (M) Representative immunohistochemistry image of commercially procured (US Biomax., Inc) TMA slides stained with ALKBH5 and DDX46 antibody, followed by a summary of respective antibody stained slides for DLBCL samples and reactive lymph nodes (LN). No staining was detected: 1, low: 2 staining density, and high: 3–4 staining density. (N) Radar chart of the Pearson correlation efficiency of stained ALKBH5 and DDX46 slides.

transcriptional RNA modifications. Understanding the role of epitranscriptomic mechanisms in B-cell activation, differentiation, and malignancy provides crucial insights into immune responses and the development of B-cell lymphomas. To investigate this, we exposed human splenic/tonsillar B-cells and cultured DLBCL cell lines (SUHDL4 and Toledo) to optimize [16] BCR mimetics and assessed global m6A RNA methylation. BCR activation led to a significant reduction in global m6A levels (Fig. 1A), coupled with increased expression of the RNA demethylase ALKBH5 and its interacting RNA helicase, DDX46, while FTO and DDX43 levels showed minimal changes. CARD11 and SYK served as internal controls [16]. ALKBH5 transcript levels were significantly elevated, whereas other gene transcripts were largely unchanged (Fig. 1B, 1 C, S1A-S1D). Transcriptomic analysis of B-cells stimulated with BCR mimetics ($n = 5$; data from GEO: GSE156195 [27]) confirmed increased ALKBH5 mRNA expression, underscoring its role in regulating BCR-mediated responses. (Fig. S1E, S1F). In vivo, C57BL/6 mice immunized with sheep red blood cells (SRBCs) [28] exhibited reduced global RNA methylation in splenic B-cells and upregulation of ALKBH5, DDX46, and CARD11. At the same time, FTO and DDX43 levels remained largely unaltered (Fig. 1d-1 G). Microscopic analysis revealed germinal center (GC) formation surrounded by a mantle and marginal zone B-cells in spleens of immunized mice, with immunohistochemistry confirming increased ALKBH5 and DDX46 expression, specifically within the GC compartment (Fig. S2A, S2B).

To evaluate the roles of ALKBH5 and DDX46 in malignant B-cells, RNA from EμMyc lymphoma tumor [29] was analyzed. Tumor-derived RNA exhibited significantly reduced m6A methylation compared to age-matched naïve splenic B-cells (Fig. 1H). Both protein and transcript analyses demonstrated elevated ALKBH5 expression in EμMyc tumors, while DDX46 upregulation was observed only at the protein level (Fig. 1I-1 M). Immunohistochemistry further revealed increased ALKBH5 and DDX46 staining in EμMyc lymphoma samples compared to wild-type spleens (Fig. S2C, S2D). Similarly, primary human DLBCL samples showed elevated ALKBH5 protein expression compared to naïve B-cells (Fig. 1L), supported by public transcriptomic datasets indicating higher ALKBH5 mRNA levels in DLBCL samples relative to normal lymphoid tissues (Supp Fig. S2E). Tissue microarrays of primary DLBCL specimens ($n = 245$) showed robust ALKBH5 and DDX46 expression in ~78 % of cases, compared to 36 % in reactive lymph nodes ($n = 35$). Pearson's correlation analysis revealed a strong positive relationship between ALKBH5 and DDX46 expression ($R^2 = 0.5149$, $p < 0.00001$) (Fig. 1M, 1 N, S2F). These findings suggest a critical role for ALKBH5 and DDX46 in modulating RNA methylation dynamics in normal and malignant B cells. Their upregulation during immune activation and in lymphoma underscores their potential as therapeutic targets in conditions characterized by dysregulated epitranscriptomic mechanisms.

Epitranscriptomic coordination of ALKBH5 and DDX46 in malignant B-Cells

Signals emanating from the BCR promote the survival of malignant B-cells, such as the heterogeneous Diffuse large B-cell lymphoma (DLBCL) [13]. Given the intrinsic heterogeneity of DLBCL, we utilized a panel of cell lines representing both ABC- and GCB-subtypes to capture the spectrum of BCR signaling dependencies. Additionally, RC, a double-hit lymphoma cell line, was included to assess the role of ALKBH5 in a genetically distinct, high-risk B-cell malignancy [30]. Genetic aberrations frequently found in DLBCL samples lead to constitutive activation of BCR signaling [9,13–15,31,32], providing an ideal context to investigate the role of ALKBH5 in regulating BCR-associated gene expression (Figure S3A). We depleted ALKBH5 or DDX46 using two independent shRNAs across a panel of BCR-addicted DLBCL cell lines. Efficient knockdown was confirmed by immunoblotting and qPCR, demonstrating robust reductions in ALKBH5 and DDX46 expression, with minimal effects on FTO and DDX43 levels. Knockdown of ALKBH5 or DDX46 led to substantial decreases in protein levels of key BCR signaling components, including CD79A, SYK, BLK, BTK, and CARD11, across all tested cell lines (Fig. 2A–C, S3B, S4, S5). CARD11, BTK, and SYK were significantly downregulated at the transcript level, whereas CD79A and BLK mRNA levels remained largely unaffected (Fig. 2C, S5). These findings point to a direct role for ALKBH5 and DDX46 in regulating essential components of the BCR signaling pathway. Chronic BCR signaling is a defining feature of several B-cell lymphomas, driving oncogenic pathways, while tonic BCR signaling supports normal B-cell survival and development [33,34]. In scrambled shRNA-transduced control DLBCL cells, treatment with BCR mimetics elevated BCR pathway genes alongside ALKBH5 and DDX46 expression. Conversely, ALKBH5 or DDX46 knockdown abrogated the upregulation of key BCR components upon activation, indicating that this demethylase complex is crucial for optimal BCR signaling (Fig. 2D, S6).

To further explore the interdependence of ALKBH5 and DDX46, we examined the expression of DDX46 upon ALKBH5 depletion in BCR-addicted DLBCL cell lines. ALKBH5 knockdown significantly reduced DDX46 protein levels without affecting its mRNA levels, while DDX43 levels were marginally altered. Similarly, DDX46 knockdown diminished ALKBH5 expression at both protein and transcript levels, while FTO expression was unaffected (Fig. 2E-2 G, S7). These findings underscore the critical role of epitranscriptomic mechanisms in modulating chronic and tonic BCR signaling in DLBCL.

ALKBH5/DDX46-Mediated m6A demethylation drives nuclear export via HuR

To further investigate the mechanisms behind epitranscriptomic regulation, we conducted an m6A RNA methylation assay, which revealed that depletion of ALKBH5 or DDX46 led to a significant increase in overall m6A methylation in DLBCL cells (Fig. 3A, S8A). To determine whether ALKBH5 and DDX46 specifically affect m6A modification, we performed methylated RNA immunoprecipitation followed by qPCR (meRIP-qPCR) for CD79A and BLK transcripts. These transcripts were selected because their expression levels remained unchanged upon ALKBH5 or DDX46 depletion, ensuring that any observed differences in m6A enrichment were not confounded by alterations in transcript abundance. This analysis demonstrated the knockdown of either ALKBH5 or DDX46 enriched m6A marks on these transcripts compared to the mock antibody group (Fig. 3B, S8B). ALKBH5 depletion decreased DDX46 protein without affecting its mRNA levels, so we hypothesized that ALKBH5 could similarly regulate DDX46 via epitranscriptomic modifications. In line with this hypothesis, ALKBH5 depletion enhanced m6A methylation on DDX46 transcripts. These findings align with our previous observation that ALKBH5 and DDX46 depletion reduces the expression of key BCR signaling components. Given the role of Human antigen R (HuR) in stabilizing BCR gene transcripts [17], enhancing their nuclear export, and promoting translation [16,17], we speculated that demethylation of these transcripts could affect their interaction with HuR. To test this, RNA immunoprecipitation (RNA-IP) with recombinant HuR revealed that HuR binding to DDX46, CD79A, and BLK transcripts was significantly reduced upon ALKBH5 or DDX46 knockdown (Fig. 3C, S8C).

To assess the subcellular dynamics of these transcripts, we performed nuclear and cytoplasmic RNA fractionation in ALKBH5/DDX46-depleted cells. The results showed nuclear retention of DDX46, CD79A, and BLK transcripts, with a concurrent decrease in their cytoplasmic levels compared to control cells (Fig. 3D, S8D). This suggests that the m6A demethylation function of the ALKBH5/DDX46 complex is crucial for efficiently exporting these mRNAs to the cytoplasm. To confirm that ALKBH5 directly regulates the m6A modification of these genes, we treated RNA purified from wild-type (C57BL/6) splenic B-cells with recombinant ALKBH5 enzyme. A dose-dependent reduction in overall m6A methylation was observed (Fig. 3E). Moreover, m6A RNA-IP and HuR-IP assays on the demethylated RNA demonstrated that ALKBH5 treatment significantly reduced the interaction of BCR

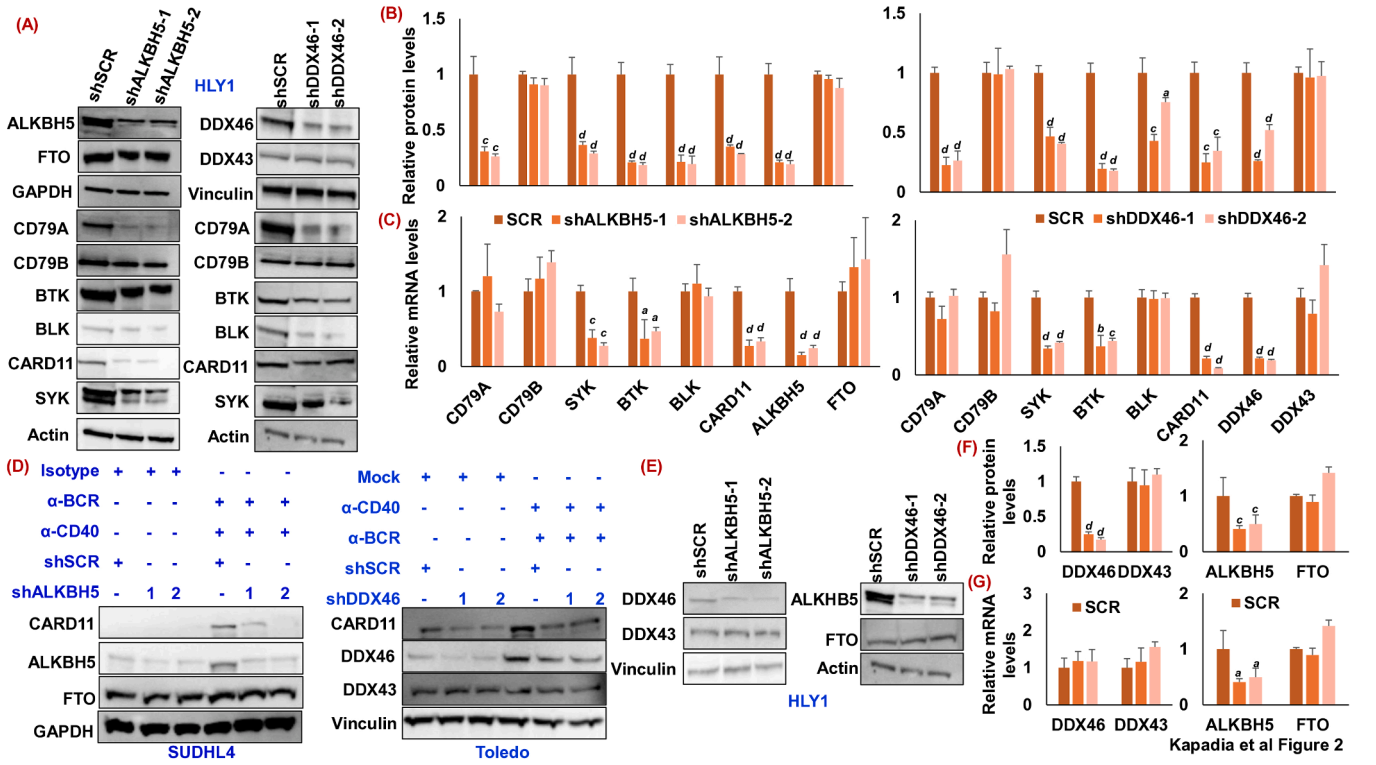

Fig. 2. Impact of ALKBH5 or DDX46 Depletion on Key B-Cell Signaling Transcripts. (A, E) Protein lysates were harvested from indicated shALKBH5 or shDDX46 stably infected DLBCL cells and were analyzed using immunoblotting with the specified antibodies. shSCR-infected cells were used as an internal control (B, F). Densitometric quantifications of immunoblots of specified antibodies from Fig. 3A and F, respectively. Values were first normalized with their respective loading controls (GAPDH, Actin, and Vinculin), neutralized with the average of shSCR infected cells, and expressed as mean ± SD, set at 1. Statistical analysis was performed using one-way ANOVA followed by Bonferroni *post hoc* analysis. $^{b}p < 0.01$, $^{c}p < 0.005$, $^{d}p < 0.001$ versus shSCR infected cells. (C, G) Total RNA was subjected to quantification of indicated genes with RT-qPCR. The results were normalized with GAPDH (reference gene), set to 1 for shSCR-infected cells, and expressed as mean ±SD. Statistical analysis was performed using one-way ANOVA followed by Bonferroni *post hoc* analysis. $^{a}p < 0.05$, $^{c}p < 0.005$, $^{d}p < 0.001$ versus shSCR infected cells. (D) Protein lysates were harvested from shALKBH5 or shDDX46 stably infected SUDHL4 or Toledo cells treated with either isotype or BCR mimetics and were analyzed using immunoblotting with the specified antibodies. shSCR-infected cells were used as an internal control.

signature transcripts (Cd79A, Blk, Btk, Card11, Syk) and Ddx46 with m6A antibodies while enhancing their binding to HuR (Fig. 3F–3 H). These findings highlight that ALKBH5-mediated m6A demethylation is essential for interacting these key transcripts with HuR, facilitating their nuclear export and stabilization in the cytoplasm, thereby promoting gene expression and signaling.

ALKBH5-DDX46 complex formation Is RNA-dependent

Two unexpected findings emerged while investigating the ALKBH5/DDX46-mediated gene regulation mechanism. First, under basal conditions, ALKBH5 was observed to co-precipitate with DDX46 (Fig. 4A). The potential influence of the intracellular nucleic acids is often overlooked in routine cellular protein interaction assessment [35]. Zheng et al. reported DDX46 precipitated ALKBH5 in the presence of vesicular stomatitis virus [36]. To determine whether the interactions were mediated by nucleic acids, immunoprecipitation was performed on nucleic acid-digested cell lysates. Precipitation of ALKBH5 with DDX46, but not of SF3B3, was significantly lost upon nuclease treatment (Benzonase) (Fig. 4B, 4 C, S9A, and S9B), indicating a potential nucleic acid-mediated interaction. Further analysis revealed that the interaction between DDX46 and ALKBH5 was hampered with RNase A treatment, but DNase I was substantially ineffective (Fig. 4D, 4 E, S9C, and S9D). Second, considering the nuclear role of m6A demethylation machinery in promoting BCR transcript translocation, we hypothesized their enhanced nuclear retention. Here, we treated lymphoblastoid cells with BCR mimetics. Lymphoblastoid cell line, served as a surrogate model for normal B-cell studies, allowing us to evaluate BCR-related transcriptional and epitranscriptomic changes in a non-malignant context [37–40]. Treating transformed B-cells (lymphoblastoid cells) with BCR mimetics unexpectedly revealed that ALKBH5 was predominantly localized in the cytoplasm. Notably, BCR activation promotes its translocation to the nucleus. Consistently [36,41], DDX46 was predominantly present in the nuclear fraction, with enhanced nuclear retention upon BCR induction (Fig. 4F, G, S9E, and S9F).

Our earlier studies showed that knockdown of ALKBH5 and DDX46 increased nuclear retention of CD79A, BLK, and DDX46 transcripts, suggesting an alteration in mRNA export upon BCR induction. To investigate this further, we performed subcellular fractionation of RNA and quantified nuclear-to-cytoplasmic transcript ratios. Consistent with our hypothesis, BCR induction significantly reduced the nuclear-to-cytoplasmic ratio of the studied transcript panel, supporting enhanced mRNA export (Fig. 4H, I, S9 G, S9H). Interestingly, ALKBH5 also regulated long non-coding RNAs (lncRNAs), such as treRNA1, which has been implicated in promoting cellular proliferation. Upon BCR induction, treRNA1 translocated from the cytoplasm to the nucleus, mirroring ALKBH5 protein behavior. Moreover, treRNA1 transcript levels were upregulated in BCR-mimetic-treated cells and depleted upon knockdown of ALKBH5 or DDX46, indicating that treRNA1 may serve as an internal regulator of the ALKBH5-DDX46 complex (Fig. 4J, K, S9I, and S9 J). These findings highlight a complex regulatory network involving ALKBH5, DDX46, and treRNA1 in controlling m6A demethylation, mRNA export, and subcellular RNA localization. It is important to note that tumor suppressor LINC01125 [42–44] lncRNA expression was noted to be upregulated upon depletion of ALKBH5 and DDX46, respectively.

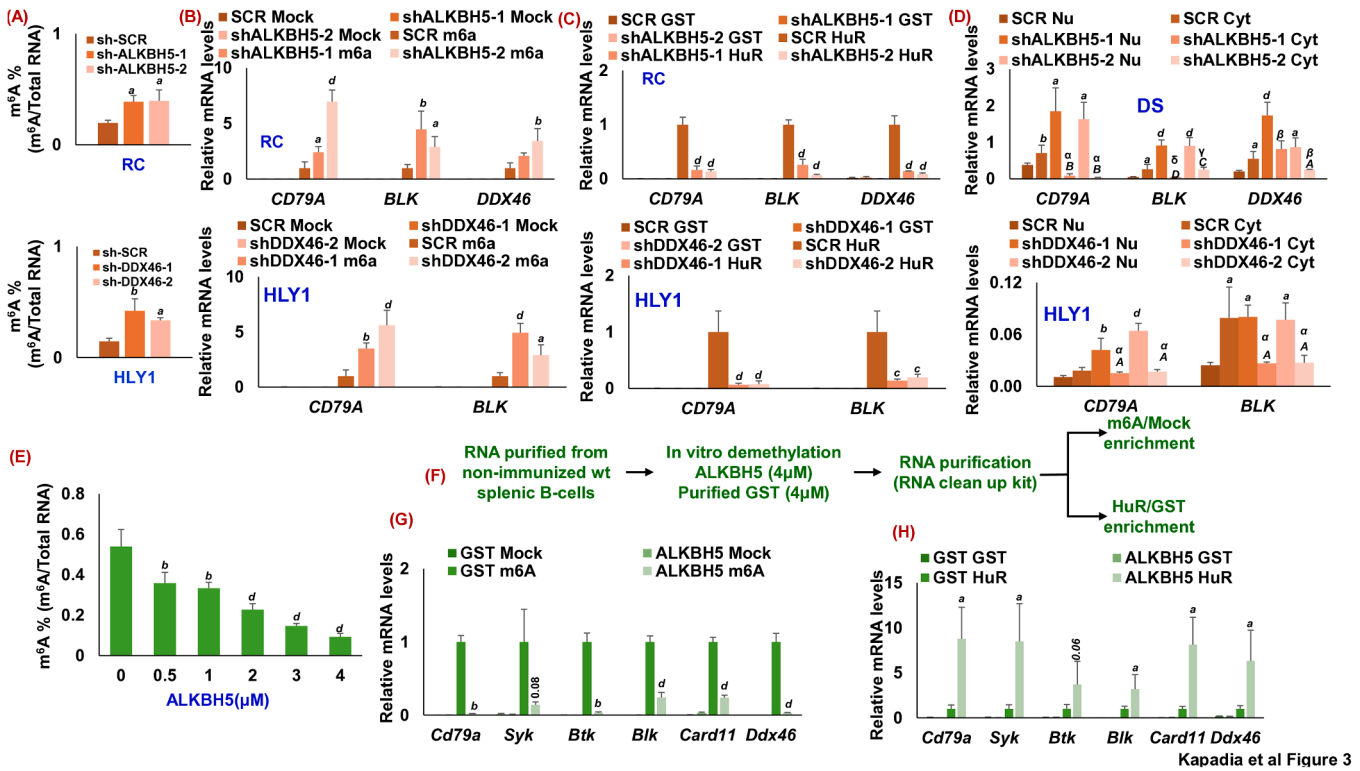

Fig. 3. Enhanced Nuclear Retention of Transcripts Upon Epitranscriptomic Disruption. (A) Total RNA was collected from shALKBH5 or shDDX46 stably infected DLBCL and shSCR infected cells and subjected to m6A quantification. The results were normalized with total RNA and expressed as mean±SD. Statistical analysis was performed using one-way ANOVA followed by Bonferroni *post hoc* analysis. $^{a}p< 0.05$ versus shSCR-infected cells. (B, C) m6A IP and HuR IP enriched RNA were subjected to RT-qPCR. Normal mouse IgG (mock) (B) and purified GST protein (C) were used as experimental controls. The results were first normalized with their respective loading controls (Luciferase mRNA) and neutralized with the average of shSCR infected cells (enriched with m6A and HuR, respectively) and expressed as mean ± SD, which was set at 1. Statistical analysis was performed using one-way ANOVA followed by Bonferroni *post hoc* analysis. $^{a}p < 0.05$, $^{b}p < 0.01$, $^{d}p < 0.001$ versus respective shSCR infected cells. (D) RT-qPCR of nuclear- and cytoplasmic-enriched fraction isolated from shALKBH5 or shDDX46 stably infected DS DLBCL and shSCR infected cells. The results were first normalized with their respective loading controls (Luciferase mRNA), neutralized with the average of shSCR infected nuclear fraction, and expressed as mean ± SD, set at 1. Statistical analysis was performed using one-way ANOVA followed by Bonferroni *post hoc* analysis. $^{a}p < 0.05$, $^{b}p < 0.01$, $^{d}p < 0.001$ versus corresponding SCR nuclear fraction, $^{B}p < 0.01$, $^{C}p < 0.005$, $^{D}p < 0.001$ versus corresponding SCR cytoplasmic fraction, $^{\alpha}p< 0.05$, $^{\gamma}p < 0.005$, $^{\delta}p < 0.001$ versus corresponding shALKBH5 nuclear fraction. (E) Commercially procured active recombinant ALKBH5 demethylated non-immunized splenic B-cell mRNA with increasing concentration. Purified GST was an experimental control. The results were normalized with total RNA and expressed as mean±SD. Statistical analysis was performed using one-way ANOVA followed by Bonferroni *post hoc* analysis. $^{b}p < 0.01$, $^{d}p < 0.001$ versus GST incubated (no ALKBH5) RNA. (F) Experimental Setup. Purified total RNA isolated from nonimmunized splenic B-cells was subjected to in vitro demethylation using recombinant ALKBH5 (4μM) or GST (4μM). RNA was purified and subjected to m6A RNA IP and HuR IP after incubation. (G, H) Quantification of m6A RT-qPCR (G) and HuR IP RT-qPCR. Mock antibody/ GST protein was used as an experimental control. The results were first normalized with their respective loading controls (Luciferase mRNA), neutralized with the average of respective total RNA, and expressed as mean ± SD, set at 1. Statistical analysis was performed using an unpaired, two-tailed Student's *t*-test. $^{a}p < 0.05$, $^{b}p < 0.01$, $^{d}p < 0.001$ vs m6A enriched GST treated RNA (G) or HuR precipitated GST treated RNA (H).

treRNA1 enhances ALKBH5 and DDX46 expression

Alteration and translocation of the lncRNA treRNA1 following BCR induction and ALKBH5/DDX46 depletion prompted us to investigate whether treRNA1 regulates the ALKBH5-DDX46-mediated BCR signaling cascade. Upon ectopic expression of treRNA1 in 293T cells, we observed a notable increase in ALKBH5 and DDX46 protein levels, whereas the expression of FTO and DDX43 showed only marginal changes (Fig. 5A, 5 B). The correlative expression along with co-dependency in the expression between ALKBH5, DDX46, and treRNA1 suggest a stronger association in functional activity. The interaction between DDX46 and ALKBH5 was hampered with the RNase A and Benzonase treatment. Moreover, BCR activation induced the nuclear translocation of treRNA1, raising the possibility that treRNA1 may serve as a molecular bridge facilitating the ALKBH5-DDX46 interaction. Using MS2-TRAP [45], ectopic expression of treRNA1 significantly enhanced the interaction between DDX46 and ALKBH5 Fig. 5C, 5 D). Conversely, the interaction between endogenous DDX46 and ALKBH5 was hampered upon transient depletion of treRNA1, with minimal impact on DDX46 and SF3B3 association (Fig. 5E, 5 F, S10A, S10B). Next, we examine the impact of treRNA1 expression on ALKBH5 translocation under BCR mimetics. It was observed that treRNA1 knockdown in BCR-activated lymphoblastoid cells significantly hampered the ALKBH5 nuclear translocation with enhanced cytoplasmic levels of DDX46 (Fig. 5G, 5 H, S10C, S10D). These findings strongly endorse the potential role of treRNA1 in the epitranscriptomic regulation of the BCR signature.

treRNA1 enhances ALKBH5-Mediated m6A demethylation

To elucidate the functional role of treRNA1 in ALKBH5-mediated demethylation activity, we first evaluated the in vitro demethylation activity of ALKBH5 in the presence of increasing concentrations of custom-synthesized, HPLC-purified treRNA1. As expected, recombinantly purified ALKBH5 effectively demethylated splenic B-cell mRNA isolated from non-immunized mice. Notably, the demethylation activity of ALKBH5 was significantly enhanced with increasing concentrations of treRNA1 (Fig. 6A). To explore the functional impact of this enhanced demethylation, we analyzed the interaction of the in vitro demethylated RNA from non-immunized splenic B cells with m6A and HuR. Supporting our hypothesis, BCR signature transcripts demethylated by the

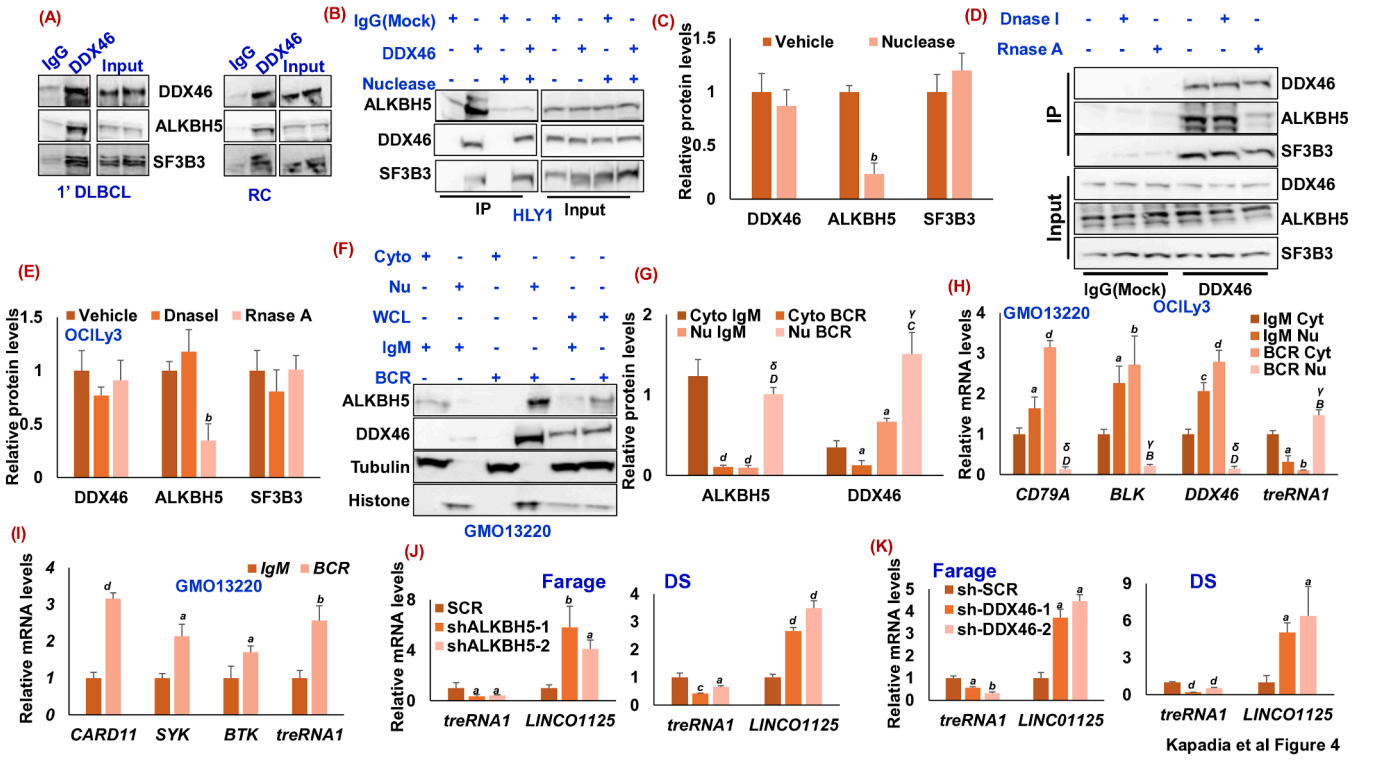

Fig. 4. DDX46 complex with ALKBH5 is sensitive to RNase treatment: (A) DDX46 Immunoprecipitation, immunoblot analysis, and whole cell lysates of indicated antibodies from primary DLBCL samples (ABC-subtype) or RC cells. (B) HLY1 protein lysates were subjected to nuclease treatment followed by DDX46 immunoprecipitation. The enriched fraction was subjected to immunoblotting with the indicated antibodies. Nuclease untreated faction (vehicle) was used as experimental control, and whole cell lysates (input) were used as internal controls. (C) Densitometric quantifications of immunoblots of indicated antibodies from Fig. B. Values were first normalized with their corresponding whole cell lysates. They were neutralized with the average DDX46-precipitated vehicle cell lysates and expressed as mean ± SD, set at 1. Statistical analysis was performed using an unpaired, two-tailed Student's *t*-test. ****$p < 0.001$ vs. Vehicle enriched fraction. (D). OCI-Ly3 lysates were subjected to either DNase I or RNase A treatment, enrichment with DDX46, and immunoblotting with indicated antibodies. Vehicle-treated lysate was used as experimental control, and whole cell lysates (input) were used as internal control. (E) Densitometric quantifications of immunoblots of indicated antibodies from Fig. D. Values were first normalized with their corresponding whole cell lysates. They were neutralized with the average DDX46-precipitated vehicle cell lysates and expressed as mean ± SD, set at 1. Statistical analysis was performed using one-way ANOVA followed by Bonferroni *post hoc* analysis. $^{b}p< 0.01$ vs. Vehicle enriched fraction. (F) GMO13220 cells were subjected to BCR mimetics treatment for 24 h, followed by nuclear-cytoplasmic fractionation. The cellular fractions and whole cell lysates were subjected to immunoblotting using indicated antibodies. Histone and Tubulin were used as an internal control for nuclear and cytoplasmic fractions, respectively. (G) Densitometric quantifications of immunoblots of indicated antibodies from Fig. F. Values were first normalized with their corresponding internal controls followed by whole cell lysates and neutralized with the average of isotype (IgM) cytoplasmic fraction and expressed as mean ± SD, which was set at 1. Statistical analysis was performed using one-way ANOVA followed by Bonferroni *post hoc* analysis. $^{b}p < 0.01$ vs. Vehicle enriched fraction. (H) RT-qPCR of the nuclear- and cytoplasmic-enriched fraction of BCR mimetics treated GMO13220 cells. The results were first normalized with their respective loading controls (Luciferase mRNA), neutralized with the average of isotype (IgM) cytoplasmic fraction, and expressed as mean ± SD, set at 1. Statistical analysis was performed using one-way ANOVA followed by Bonferroni *post hoc* analysis. $^{a}p< 0.05$, $^{b}p < 0.01$, $^{d}p < 0.001$ versus corresponding SCR nuclear fraction, $^{B}p < 0.01$, $^{C}p < 0.005$, $^{D}p < 0.001$ versus corresponding SCR cytoplasmic fraction, $^{\alpha}p < 0.05$, $^{\gamma}p < 0.005$, $^{\delta}p < 0.001$ versus corresponding shDDX46 nuclear fraction. (I) Total RNA isolated from BCR mimetics-treated GMO13220 cells was subjected to quantification of indicated genes with RT-qPCR. The results were normalized with GAPDH (reference gene), set to 1 for isotype (IgM) treated cells. Statistical analysis was performed using an unpaired, two-tailed Student's *t*-test. $^{a}p < 0.05$, $^{b}p < 0.01$, $^{d}p < 0.001$ vs IgM treated cells. (J, K) Total RNA isolated from shALKBH5 (J) or shDDX46 (K) stably infected DLBCL cells were subjected to quantification of indicated genes with RT-qPCR. The results were normalized with GAPDH (reference gene), set to 1 for shSCR-infected cells, and expressed as mean±SD. Statistical analysis was performed using one-way ANOVA followed by Bonferroni *post hoc* analysis. $^{a}p < 0.05$, $^{b}p < 0.01$, $^{d}p < 0.001$ versus corresponding shSCR infected cells.

ALKBH5-treRNA1 complex exhibited reduced m6A antibody binding and increased interaction with purified HuR protein (Fig. 6B, 6 C).

To investigate the dependency of ALKBH5 and DDX46 expression on treRNA1, we transduced DLBCL cell lines with shRNA targeting treRNA1. Quantitative analysis confirmed the successful depletion of treRNA1, which was accompanied by an increased expression of the lncRNA LINC01125 (Fig. 6D, S10E). Immunoblotting revealed a significant reduction in ALKBH5 and DDX46 protein levels, while FTO and DDX43 levels remained largely unaffected (Fig. 6E, 6 F, S11A, S11B). Only ALKBH5 showed altered expression at the transcript level, whereas FTO, DDX46, and DDX43 transcripts remained unchanged (Fig. 6G, S11C).

Given the observed dependency of demethylation on treRNA1, we measured overall m6A levels in RNA isolated from treRNA1-depleted cells. As anticipated, treRNA1 depletion significantly reduced global m6A methylation levels (Fig. 6H, S11D). To assess the role of treRNA1 in the epitranscriptomic regulation of the BCR signature, we analyzed m6A enrichment and HuR interactions for BCR signature transcripts. TreRNA1 knockdown enhanced m6A enrichment on DDX46, CD79A, and BLK transcripts (Fig. 6I, S11E), increased their nuclear retention (Fig. 6J, S11F), and reduced their complex formation with HuR (Fig. 6K, S11 G). Furthermore, we evaluated the impact of treRNA1 knockdown on BCR protein and transcript levels. While BCR protein expression and transcript levels were generally impaired in treRNA1-depleted cells, CD79B expression and mRNA levels were comparable to controls (Fig. 6l-6 N, S12A-S12C). We exposed non-BCR cell lines to BCR mimetics to extend our findings and assess protein induction. Consistent with our earlier observations, treRNA1 depletion markedly reduced the protein levels of SYK and CARD11 upon BCR mimetic stimulation (Fig. 6O, S12D, S12E). Finally, we confirmed that ALKBH5 and DDX46

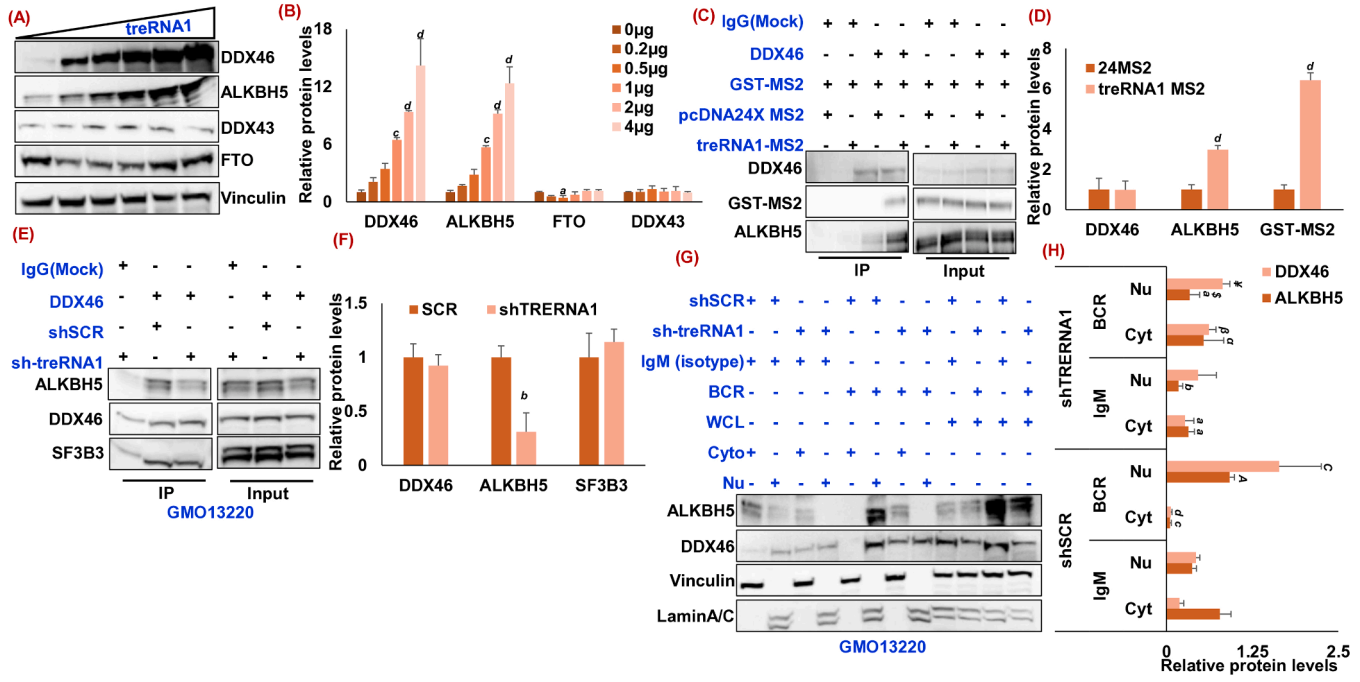

Kapadia et al Figure 5

Fig. 5. treRNA1 is molecular glue between DDX46 and ALKBH5. (A) 293T cells were transfected with increasing concentrations of treRNA1. After 48 h of transfection, cellular lysates were subjected to immunoblotting using the indicated proteins. (B) Densitometric quantification of Fig. A. GFP transfection was used as an experimental control. Values were first normalized with their corresponding loading control (Vinculin), neutralized with the average of GFP transfected cells (treRNA1 0µg), and expressed as mean ± SD, set at 1. Statistical analysis was performed using one-way ANOVA followed by Bonferroni *post hoc* analysis. $^{a}p< 0.05$, $^{c}p< 0.005$, $^{d}p< 0.001$ versus 0µg transfected cells. (C) 293T cells were transfected with treRNA1-24 MS2 in presence of MS2-GST. After 24 h of transfection, cellular lysates were subjected to enrichment with DDX46. Immunoblotting analysis was pursued with indicated antibodies. Empty 245X MS2 construct with MS2-GST expression construct was used as an experimental control. Whole-cell lysates were used as internal controls. (D) Densitometric quantifications of immunoblots of indicated antibodies from Fig. C. Values were first normalized with their corresponding whole cell lysates and neutralized with the average of DDX46-precipitated 24MS2 cell lysates and expressed as mean ± SD, which was set at 1. Statistical analysis was performed using an unpaired, two-tailed Student's *t*-test. $^{d}p<0.001$ vs 24MS2 enriched fraction. (E) GMO13220 cells were transiently infected with shTRERNA1 or shSCR. 24 h post-infection, cellular lysates were subjected to enrichment with DDX46. Immunoblotting analysis was pursued with indicated antibodies. Empty 245X MS2 construct with MS2-GST expression construct was used as an experimental control. Whole-cell lysates were used as internal controls. (F) Densitometric quantifications of immunoblots of indicated antibodies from Fig. E. Values were first normalized with their corresponding whole cell lysates and neutralized with the average of DDX46-precipitated shSCR cell lysates and expressed as mean ± SD, which was set at 1. Statistical analysis was performed using an unpaired, two-tailed Student's *t*-test. $^{b}p < 0.01$ vs SCR-enriched fraction. (G) GMO13220 cells transiently infected with shTRERNA1 were subjected to BCR mimetic treatment for 24h. Cells were subjected to cellular fractionation and immunoblotting with indicated antibodies after treatment. Isotype (IgM) treatment was used to control BCR mimetics—shSCR infection for shTRERNA1 and whole cell lysates for cellular fractionation. Vinculin and LaminA/C were used as internal controls for cytoplasmic and nuclear fractions. (H) Densitometric quantifications of immunoblots of indicated antibodies from Fig. G. Values were first normalized with their corresponding internal controls followed by whole cell lysates and neutralized with the average of isotype (IgM) cytoplasmic fraction and expressed as mean ± SD, which was set at 1. Statistical analysis was performed using one-way ANOVA followed by Bonferroni *post hoc* analysis. $^{b}p < 0.01$ vs. Vehicle enriched fraction.

are induced upon BCR activation, and their expression is significantly reduced upon treRNA1 knockdown in the context of BCR activation (Figs. 6O, S12F, S12 G). Collectively, these findings establish the critical role of the ALKBH5-treRNA1-DDX46 axis in regulating the BCR signature. Disruption of this regulatory axis significantly attenuates the BCR signaling pathway in DLBCL, highlighting its therapeutic potential.

Discussion

Epitranscriptomics has gained relevance, especially with advancements in techniques for studying RNA modifications, notably N6-methyladenosine (m6A), the most prevalent modification in mRNA. This modification plays important roles in many physiological processes and is implicated in numerous disease states, including cancer [18]. In tumor cells' epitranscriptomic homeostasis is disrupted to promote cancer-prone features, by the machinery of writers, readers, and erasers [46–49]. Although, m6A has been explored in many perspectives and different contexts in the past few years [50–52], its role in immune development especially in B-cell biology is poorly understood. Here, we demonstrate the role of mRNA methylation in augmenting the BCR expression that is critical for germinal center formation [7,34,53,54] and tumor development/progression [4,9,10,14,16,17,32,55–58] along with tumor vascularization [59–61]. We observed that the activated B-cells, most notably with BCR mimetics, exhibit a substantial decrease in overall m6A levels. Simultaneously, crucial elements of the demethylase apparatus: ALKBH5, DDX46, and the novel regulator treRNA1, exhibit strong nuclear localization and increased expression. Together, these findings portray the emergence of a new protein-RNA complex that facilitates efficient translocation and translation for optimal BCR functionality of essential BCR signature genes.

In the last few years, biological and clinical studies in antitumor response have highlighted the multifaceted role of B-cells in tumor biology [3]. Although controversial, several independent studies using clinical datasets have demonstrated that non-tumorous B-cells in the tumor microenvironment can influence the response to cancer therapy [62–64]. Pre-clinical studies using BCR inhibitors displayed positive

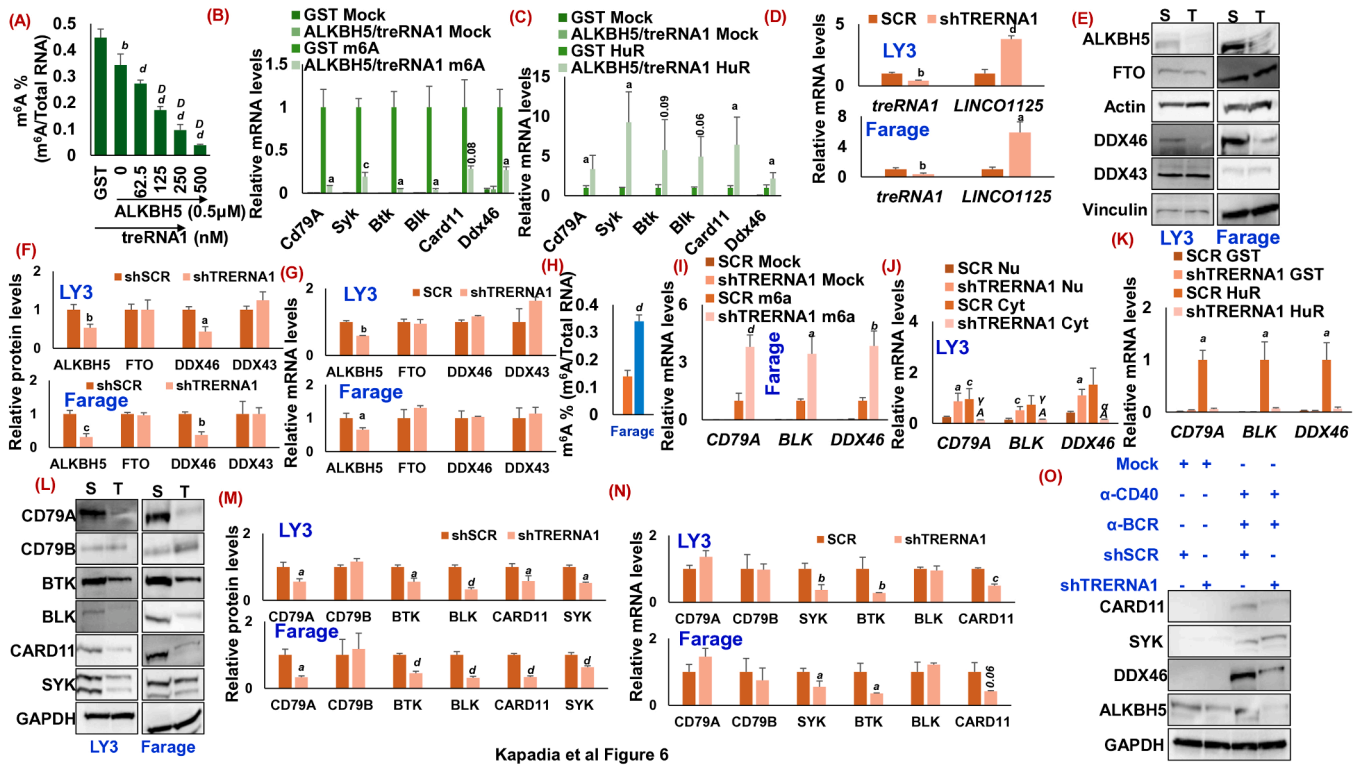

Fig. 6. treRNA1 enhances ALKBH5 demethylase activity: (A) Commercially procured active recombinant ALKBH5 in the presence of an increasing concentration of HPLC purified treRNA1 demethylated non-immunized splenic B-cell mRNA. Purified GST was an experimental control. The results were normalized with total RNA and expressed as mean±SD. Statistical analysis was performed using one-way ANOVA followed by Bonferroni *post hoc* analysis. $^{b}p < 0.01$, $^{d}p < 0.001$ versus GST incubated (no ALKBH5) RNA. $^{D}p < 0.001$ versus ALKBH5 0.5μM (no treRNA1). (B, C) Quantification of m6A RT-qPCR (G) and HuR IP RT-qPCR of demethylated non-immunized splenic B-cell mRNA. Mock antibody/ GST protein was used as the experimental control. The results were first normalized with their respective loading controls (Luciferase mRNA), neutralized with the average of respective total RNA, and expressed as mean ± SD, set at 1. Statistical analysis was performed using an unpaired, two-tailed Student's *t*-test. $^{a}p < 0.05$ vs m6A enriched GST treated RNA (B) or HuR precipitated GST treated RNA (C). (D, G, N) Total RNA isolated from shTRERNA1 stably infected DLBCL cells were subjected to quantification of indicated genes with RT-qPCR. The results were normalized with GAPDH (reference gene), set to 1 for shSCR-infected cells, and expressed as mean ± SD. Statistical analysis was performed using an unpaired, two-tailed Student's *t*-test. $^{a}p < 0.05$, $^{b}p < 0.01$, $^{d}p < 0.001$ versus corresponding shSCR infected cells. (E, L) Protein lysates were harvested from indicated shTRERNA1 stably infected DLBCL cells and were analyzed using immunoblotting with the specified antibodies. shSCR infected cells were used as internal control; S: shSCR, T: shTRERNA1 (F, M) Densitometric quantifications of immunoblots of specified antibodies from Fig. E and L, respsectively. Values were first normalized with their respective loading controls and neutralized with the average of shSCR infected cells and expressed as mean ± SD, which was set at 1. Statistical analysis was performed using an unpaired, two-tailed Student's *t*-test. $^{a}p < 0.05$, $^{b}p < 0.01$, $^{c}p < 0.005$ versus corresponding shSCR infected cells. (H) Total RNA was collected from shTRERNA1 stably infected Farage cells along with shSCR infected cells and subjected to m6A quantification. The results were normalized with total RNA and expressed as mean±SD. Statistical analysis was performed using an unpaired, two-tailed Student's *t*-test. $^{d}p < 0.001$ versus corresponding shSCR-infected cells. (I, K) m6A IP and HuR IP enriched RNA were subjected to RT-qPCR. Normal mouse IgG (mock) (I) and purified GST protein (K) were used as experimental controls. The results were first normalized with their respective loading controls (Luciferase mRNA) and neutralized with the average of shSCR infected cells (enriched with m6A and HuR, respectively) and expressed as mean ± SD, which was set at 1. Statistical analysis was performed using an unpaired, two-tailed Student's *t*-test. $^{a}p < 0.05$, $^{b}p < 0.01$, $^{d}p < 0.001$ versus corresponding shSCR infected cells. (J) RT-qPCR of nuclear- and cytoplasmic-enriched fraction isolated from shDDX46 stably infected DLBCL and shSCR infected cells. The results were first normalized with their respective loading controls (Luciferase mRNA), neutralized with the average of shSCR infected nuclear fraction, and expressed as mean ± SD, set at 1. Statistical analysis was performed using one-way ANOVA followed by Bonferroni *post hoc* analysis. $^{a}p < 0.05$, $^{b}p < 0.01$, $^{d}p < 0.001$ versus corresponding SCR nuclear fraction, $^{B}p < 0.01$, $^{c}p < 0.005$, $^{D}p < 0.001$ versus corresponding SCR cytoplasmic fraction, $^{\alpha}p < 0.05$, $^{\gamma}p < 0.005$, $^{\delta}p < 0.001$ versus corresponding shDDX46 nuclear fraction. (O) Protein lysates were harvested from shTRERNA1 stably infected Toledo cells treated with either isotype or BCR mimetics and were analyzed using immunoblotting with the specified antibodies. shSCR infected cells were used as internal control.

outcomes in solid cancer [65,66], indicating BCR signature genes may be potential targets in impacting harmful tumor growth. Given the modest clinical responses of the current BCR inhibitors, there is a critical need to expand our understanding of BCR regulation and identify new druggable targets. Similarly, analysis of the publicly available datasets [27] verified that the ALKBH5 transcripts levels are frequently upregulated, including those of the primary lymphoma samples. This study validates the functional role of ALKBH5 in augmenting BCR signature and a tumor-promoting role in DLBCL through RNA interference. ALKBH5 knockdown demonstrated a robust reduction in BCR signature gene expression (except CD79B). Critically, our *in vitro* studies demonstrated that ALKBH5 directly demethylates BCR signature transcripts, hijacking the post-transcriptional/translational regulation of gene expression, crucial for normal B-cell development and lymphomagenesis. Consistent with our report [67], both protein and transcript levels of ALKBH5 were enhanced in human and rodent tumor samples. Clinical datasets predict that ALKBH5 expression correlates with poor patient survival as it promotes PD-L1-mediated immune escape [68–70]. Indeed, pan-cancer analysis indicates that ALKBH5 is a potential prognostic and immunotherapeutic biomarker for numerous cancers [71]. Our study indicates that molecular targeting of ALKBH5 may overcome the immunotherapeutic resistance, in part, by curtailing the BCR signature.

Our study suggests a distinct mechanism of DDX46-mediated BCR regulation and lymphoma growth. In agreement with Zheng et al. [36], we noted DDX46 form complex with ALKBH5 to remove the m^6A

residues from the BCR transcript. Hijacking this event retains BCR transcript in the nucleus and hampers their gene expression. The subcellular mobility of the mRNA has an important role in the gene expression regulation and in-depth analysis is warranted to evaluate epi transcriptomic's role for this intrinsic movement [72]. In part, we noted the m6A levels of BCR transcript govern its interaction with HuR [17] and thus nuclear transport. Unexpectedly, we came upon a crucial observation. Evaluating the DDX46 gene expression regulation under BCR mimetic conditions, similar to BCR signature genes, alteration of the overall m6A levels of the helicase's transcript modifies its interaction with HuR leading to nuclear export. Of relevance, Silanes et al. also predicted that HuR directly regulates DDX46 expression in colon cancer [73]. Independently, this observation indicates a feedforward loop-mediated BCR signaling regulation. Similarly, the protein levels of DDX46 were independent of its mRNA levels revealing epitranscriptomic modulation as a major form of its regulation. In addition, DDX46 is a member of the multiprotein complex and is involved in the physiological process of mRNA splicing and ribosome assembly and is critical for hematopoietic development and immunity [36,74–76]. Several studies have also reported the altered expression of DDX46 in numerous cancers [41,77,78]. Our finding that DDX46 is critical for the BCR signature further supports the mounting evidence that the protein is an oncogenic effector contributing to tumor progression. Future studies should investigate the potential implication of DDX46 in tumor development, immunotherapy, and anti-tumor resistance.

While searching for the mechanism by which ALKBH5-DDX46 regulates the BCR signature, we determined that treRNA1 bridges the complex in a *trans* manner. While, treRNA1 has been reported to be upregulated in DLBCL with a positive correlation with ALKBH5 [67], the current study delves deeper into its functional role. The findings demonstrate that treRNA1, upon BCR induction, translocates ALKBH5 into the nucleus and enhances its demethylation activity. Importantly, treRNA1 depletion is strongly correlated with notable suppression of BCR signature gene expression highlighting the potential significance of targeting treRNA1 as a pivotal element for augmenting immunotherapeutic approaches in DLBCL. Indeed, several studies report that enhanced expression of treRNA1 augments the metastatic properties of the tumorous cells, indicating the lncRNA, independent of tumor origin, plays a dominant role in altering the tumor microenvironment facilitating the cancer cell migration [79–81]. Along with the BCR signature, treRNA1 is reported to regulate metastatic markers including E-cadherin [82], CDH1 [83], and SNAI [79]. To point, treRNA1 is a tumor-oncogenic lncRNA.

Despite extensive research on the roles and underlying molecular mechanisms of RNA m6A modification in cancer, many unanswered questions remain. The observation that both m6A writers like METTL3 and erasers like ALKBH5 display similar roles in the same cancer type raises intriguing questions about the complex and context-dependent nature of m6A modification in cancer biology [6,67,84]. Quantitative, site-specific analysis of m6A alterations may help unravel the complexities associated with the overlapping roles of writers and erasers. We previously established that BCR signatures like CARD11 are dependent upon eIF4A activity [16]. Recent reports suggest that under duress eIF3D mediated translational regulation is achieved for ALKBH5-sensitive transcript [85]. The interplay between the epitranscriptiomic and the translational apparatus including eIF4A and eIF3D highlights the need for a comprehensive understanding of how m6A modifications contribute to gene expression. In this manuscript, we demonstrated that the activity of ALKBH5 is enhanced with interactions/complex formation with DDX46 and treRNA1. Moreover post-translation modifications of ALKBH5, like ubiquitination and acetylation alter its functionality/stability [86–88]. Exploring the impact of classical oncogenic signaling pathways, including the mTOR pathway, on m6A machinery could provide additional insights into the regulatory mechanisms. This knowledge could pave the way for the development of targeted therapeutic strategies based on m6A regulation.

Funding

The Virginia Commonwealth University Flow Cytometry, Cancer Mouse Models, and Microscopy Shared Resource generated services and products supporting the research project, which was supported, in part, with funding from the NIH—NCI Cancer Center Support Grant P30 CA016059. BK and RBG are supported by VA Review Merit. BK is also supported by the RIVR Pilot Grant (MRI2022-01).

Data availability

All the supporting data for this study are available from the corresponding author on reasonable request.

CRediT authorship contribution statement

Bandish Kapadia: Writing – review & editing, Writing – original draft, Visualization, Validation, Resources, Methodology, Investigation, Funding acquisition, Formal analysis, Data curation, Conceptualization. **Anirban Roychowdhury:** Writing – review & editing, Visualization, Formal analysis, Data curation. **Forum Kayastha:** Writing – review & editing, Methodology, Formal analysis, Data curation. **Won Sok Lee:** Visualization, Formal analysis. **Nahid Nanaji:** Formal analysis, Data curation. **Jolene Windle:** Formal analysis. **Ronald Gartenhaus:** Writing – review & editing, Supervision, Conceptualization, Funding acquisition.

Declaration of competing interest

The authors declare that they have no known competing financial interests or personal relationships that could have appeared to influence the work reported in this paper.

Acknowledgments

BK and RBG appreciate helpful comments from the Richmond VAMC Cancer Center members. The authors would like to thank the Pathology and Animal Core facility at Richmond VAMC for their support and Drs. Myriam Gorospe, Ari Melnick, David Root, and Didier Trono for generous access to reagents.

Supplementary materials

Supplementary material associated with this article can be found, in the online version, at doi:10.1016/j.neo.2025.101144.

References

[1] M. Akkaya, K. Kwak, S.K. Pierce, B cell memory: building two walls of protection against pathogens, Nat. Rev. Immunol. 20 (2020) 229–238.
[2] D.G. Efremov, S. Turkalj, L. Laurenti, Mechanisms of B cell receptor activation and responses to B cell receptor inhibitors in B cell malignancies, Cancers (Basel) 12 (2020).
[3] A. Sarvaria, J.A. Madrigal, A. Saudemont, B cell regulation in cancer and anti-tumor immunity, Cell Mol. Immunol. 14 (2017) 662–674.
[4] N. Profitos-Peleja, J.C. Santos, A. Marin-Niebla, G. Roue, M.L. Ribeiro, Regulation of B-cell receptor signaling and its therapeutic relevance in aggressive B-cell lymphomas, Cancers (Basel) 14 (2022).
[5] J.A. Jones, J.C. Byrd, How will B-cell-receptor-targeted therapies change future CLL therapy? Blood 123 (2014) 1455–1460.
[6] L. Feng, Q. Yan, H. Pan, W. Shi, METTL3 enhances the effect of YTHDF1 on NEDD1 mRNA stability by m6A modification in diffuse large B-cell lymphoma cells, Immun. Inflamm. Dis. 11 (2023) e789.
[7] H. Huang, G. Zhang, G.X. Ruan, Y. Li, W. Chen, J. Zou, R. Zhang, J. Wang, S.J. Ji, S. Xu, et al., Mettl14-Mediated m6A modification is essential for germinal center B cell response, J. Immunol. 208 (2022) 1924–1936.
[8] A. Grenov, H. Hezroni, L. Lasman, J.H. Hanna, Z. Shulman, YTHDF2 suppresses the plasmablast genetic program and promotes germinal center formation, Cell Rep. 39 (2022) 110778.

[9] R.M. Young, J.D. Phelan, W.H. Wilson, L.M. Staudt, Pathogenic B-cell receptor signaling in lymphoid malignancies: new insights to improve treatment, Immunol. Rev. 291 (2019) 190–213.
[10] J.A. Woyach, A.J. Johnson, J.C. Byrd, The B-cell receptor signaling pathway as a therapeutic target in CLL, Blood 120 (2012) 1175–1184.
[11] Y. Wen, Y. Jing, L. Yang, D. Kang, P. Jiang, N. Li, J. Cheng, J. Li, X. Li, Z. Peng, et al., The regulators of BCR signaling during B cell activation, Blood Sci. 1 (2019) 119–129.
[12] V. Seda, M. Mraz, B-cell receptor signalling and its crosstalk with other pathways in normal and malignant cells, Eur. J. Haematol. 94 (2015) 193–205.
[13] R.M. Young, L.M. Staudt, Targeting pathological B cell receptor signalling in lymphoid malignancies, Nat. Rev. Drug Discov. 12 (2013) 229–243.
[14] R.E. Davis, V.N. Ngo, G. Lenz, P. Tolar, R.M. Young, P.B. Romesser, H. Kohlhammer, L. Lamy, H. Zhao, Y. Yang, et al., Chronic active B-cell-receptor signalling in diffuse large B-cell lymphoma, Nature 463 (2010) 88–92.
[15] W.H. Wilson, R.M. Young, R. Schmitz, Y. Yang, S. Pittaluga, G. Wright, C.J. Lih, P. M. Williams, A.L. Shaffer, J. Gerecitano, et al., Targeting B cell receptor signaling with ibrutinib in diffuse large B cell lymphoma, Nat. Med. 21 (2015) 922–926.
[16] J.J. Steinhardt, R.J. Peroutka, K. Mazan-Mamczarz, Q. Chen, S. Houng, C. Robles, R.N. Barth, J. DuBose, B. Bruns, R. Tesoriero, et al., Inhibiting CARD11 translation during BCR activation by targeting the eIF4A RNA helicase, Blood 124 (2014) 3758–3767.
[17] B. Dai, A.Y. Chen, C.P. Corkum, R.J. Peroutka, A. Landon, S. Houng, P. A. Muniandy, Y. Zhang, E. Lehrmann, K. Mazan-Mamczarz, et al., Hepatitis C virus upregulates B-cell receptor signaling: a novel mechanism for HCV-associated B-cell lymphoproliferative disorders, Oncogene 35 (2016) 2979–2990.
[18] R. Gao, M. Ye, B. Liu, M. Wei, D. Ma, K. Dong, m6A Modification: a double-edged sword in Tumor development, Front. Oncol. 11 (2021) 679367.
[19] X. Jiang, B. Liu, Z. Nie, L. Duan, Q. Xiong, Z. Jin, C. Yang, Y. Chen, The role of m6A modification in the biological functions and diseases, Signal. Transduct. Target. Ther. 6 (2021) 74.
[20] J. Pan, T. Huang, Z. Deng, C. Zou, Roles and therapeutic implications of m6A modification in cancer immunotherapy, Front. Immunol. 14 (2023) 1132601.
[21] X.Y. Chen, J. Zhang, J.S. Zhu, The role of m(6)A RNA methylation in human cancer, Mol. Cancer 18 (2019) 103.
[22] A.C. Grenov, L. Moss, S. Edelheit, R. Cordiner, D. Schmiedel, A. Biram, J.H. Hanna, T.H. Jensen, S. Schwartz, Z. Shulman, The germinal center reaction depends on RNA methylation and divergent functions of specific methyl readers, J. Exp. Med. (2021) 218.
[23] C. Jiang, S.J. Trudeau, T.-C. Cheong, R. Guo, M. Teng, L.W. Wang, Z. Wang, C. Pighi, C. Gautier-Courteille, Y. Ma, CRISPR/Cas9 screens reveal multiple layers of B cell CD40 regulation, Cell Rep. 28 (1307–1322) (2019) e1308.
[24] K.Y. Su, A. Watanabe, C.H. Yeh, G. Kelsoe, M. Kuraoka, Efficient culture of Human naive and memory B cells for use as APCs, J. Immunol. 197 (2016) 4163–4176.
[25] C.L. Xiao, S. Zhu, M. He, D. Chen, Q. Zhang, Y. Chen, G. Yu, J. Liu, S.Q. Xie, F. Luo, et al., N(6)-methyladenine DNA modification in the human genome, Mol. Cell 71 (2018) 306–318, e307.
[26] S. Zhang, B.S. Zhao, A. Zhou, K. Lin, S. Zheng, Z. Lu, Y. Chen, E.P. Sulman, K. Xie, O. Bogler, et al., m(6)A demethylase ALKBH5 maintains tumorigenicity of glioblastoma stem-like cells by sustaining FOXM1 expression and cell proliferation program, Cancer Cell 31 (2017) 591–606, e596.
[27] M. Syedbasha, F. Bonfiglio, J. Linnik, C. Stuehler, D. Wuthrich, A. Egli, Interferon-lambda enhances the differentiation of naive B cells into plasmablasts via the mTORC1 pathway, Cell Rep. 33 (2020) 108211.
[28] E.J. McAllister, J.R. Apgar, C.R. Leung, R.C. Rickert, J. Jellusova, New methods to analyze B cell immune responses to Thymus-dependent antigen sheep red blood, Cells *J Immunol* 199 (2017) 2998–3003.
[29] M. Lefebure, R.W. Tothill, E. Kruse, E.D. Hawkins, J. Shortt, G.M. Matthews, G. P. Gregory, B.P. Martin, M.J. Kelly, I. Todorovski, et al., Genomic characterisation of Emu-Myc mouse lymphomas identifies Bcor as a Myc co-operative tumour-suppressor gene, Nat. Commun. 8 (2017) 14581.
[30] L.V. Pham, G. Lu, A.T. Tamayo, J. Chen, P. Challagundla, J.L. Jorgensen, L. J. Medeiros, R.J. Ford, Establishment and characterization of a novel MYC/BCL2 "double-hit" diffuse large B cell lymphoma cell line, RC, J. Hematol. Oncol. 8 (2015) 121.
[31] C.G.K. Ziegler, J. Kim, K. Piersanti, A. Oyler-Yaniv, K.V. Argyropoulos, M.R.M. van den Brink, M.L. Palomba, N. Altan-Bonnet, G. Altan-Bonnet, Constitutive activation of the B cell receptor underlies dysfunctional signaling in chronic lymphocytic leukemia, Cell Rep. 28 (2019) 923–937, e923.
[32] 3rd R.M. Young, A.L. Shaffer, J.D. Phelan, L.M. Staudt, B-cell receptor signaling in diffuse large B-cell lymphoma, Semin. Hematol. 52 (2015) 77–85.
[33] W. Liu, P. Tolar, W. Song, T.J. Kim, Editorial: BCR signaling and B cell activation, Front. Immunol. 11 (2020) 45.
[34] J.C. Yam-Puc, L. Zhang, Y. Zhang, K.M. Toellner, Role of B-cell receptors for B-cell development and antigen-induced differentiation, F1000Res. 7 (2018) 429.
[35] T.N. Nguyen, J.A. Goodrich, Protein-protein interaction assays: eliminating false positive interactions, Nat. Methods 3 (2006) 135–139.
[36] Q. Zheng, J. Hou, Y. Zhou, Z. Li, X. Cao, The RNA helicase DDX46 inhibits innate immunity by entrapping m(6)A-demethylated antiviral transcripts in the nucleus, Nat. Immunol. 18 (2017) 1094–1103.
[37] L. Bai, Y. Xiang, M. Tang, S. Liu, Q. Chen, Q. Chen, M. Zhang, S. Wan, Y. Sang, Q. Li, et al., ALKBH5 controls the meiosis-coupled mRNA clearance in oocytes by removing the N (6)-methyladenosine methylation, Nat. Commun. 14 (2023) 6532.
[38] G. Zheng, J.A. Dahl, Y. Niu, P. Fedorcsak, C.M. Huang, C.J. Li, C.B. Vagbo, Y. Shi, W.L. Wang, S.H. Song, et al., ALKBH5 is a mammalian RNA demethylase that impacts RNA metabolism and mouse fertility, Mol. Cell 49 (2013) 18–29.
[39] C. Tang, R. Klukovich, H. Peng, Z. Wang, T. Yu, Y. Zhang, H. Zheng, A. Klungland, W. Yan, ALKBH5-dependent m6A demethylation controls splicing and stability of long 3′-UTR mRNAs in male germ cells, Proc. Natl. Acad. Sci. US.A 115 (2018) E325–E333.
[40] T. Du, G. Li, J. Yang, K. Ma, RNA demethylase Alkbh5 is widely expressed in neurons and decreased during brain development, Brain Res. Bull. 163 (2020) 150–159.
[41] Q. Lin, H.J. Jin, D. Zhang, L. Gao, DDX46 silencing inhibits cell proliferation by activating apoptosis and autophagy in cutaneous squamous cell carcinoma, Mol. Med. Rep. 22 (2020) 4236–4242.
[42] J. Guo, H. Pan, Long noncoding RNA LINC01125 enhances cisplatin sensitivity of ovarian cancer via miR-1972, Med. Sci. Monit. 25 (2019) 9844–9854.
[43] W. Wan, Y. Hou, K. Wang, Y. Cheng, X. Pu, X. Ye, The LXR-623-induced long non-coding RNA LINC01125 suppresses the proliferation of breast cancer cells via PTEN/AKT/p53 signaling pathway, Cell Death. Dis. 10 (2019) 248.
[44] H. Lan, J. Yuan, D. Zeng, C. Liu, X. Guo, J. Yong, X. Zeng, S. Xiao, The emerging role of non-coding RNAs in drug resistance of ovarian cancer, Front. Genet. 12 (2021) 693259.
[45] J.H. Yoon, M. Gorospe, Identification of mRNA-interacting factors by MS2-TRAP (MS2-Tagged RNA Affinity Purification), Methods Mol. Biol. 1421 (2016) 15–22.
[46] J. Lobo, D. Barros-Silva, R. Henrique, C. Jeronimo, The emerging role of Epitranscriptomics in cancer: focus on urological tumors, Genes (Basel) (2018) 9.
[47] B.J. Petri, C.M. Klinge, m6A readers, writers, erasers, and the m6A epitranscriptome in breast cancer, J. Mol. Endocrinol. (2023) 70.
[48] H. Lian, Q.H. Wang, C.B. Zhu, J. Ma, W.L. Jin, Deciphering the epitranscriptome in cancer, Trends. Cancer 4 (2018) 207–221.
[49] S.H. Han, J. Choe, Deciphering the molecular mechanisms of epitranscriptome regulation in cancer, BMB Rep. 54 (2021) 89–97.
[50] Z. Liu, L. Gao, L. Cheng, G. Lv, B. Sun, G. Wang, Q. Tang, The roles of N6-methyladenosine and its target regulatory noncoding RNAs in tumors: classification, mechanisms, and potential therapeutic implications, Exp. Mol. Med. 55 (2023) 487–501.
[51] Li C., Liu L., Li S., Liu Y.S. (2023). N6-Methyladenosine in vascular aging and related diseases: clinical perspectives *aging dis*.
[52] G. Jia, Y. Fu, X. Zhao, Q. Dai, G. Zheng, Y. Yang, C. Yi, T. Lindahl, T. Pan, Y. G. Yang, et al., N6-methyladenosine in nuclear RNA is a major substrate of the obesity-associated FTO, Nat. Chem. Biol. 7 (2011) 885–887.
[53] A.M. Khalil, J.C. Cambier, M.J. Shlomchik, B cell receptor signal transduction in the GC is short-circuited by high phosphatase activity, Science (1979) 336 (2012) 1178–1181.
[54] K. Huse, B. Bai, V.I. Hilden, L.K. Bollum, T.K. Vatsveen, L.A. Munthe, E.B. Smeland, J.M. Irish, S. Walchli, J.H. Myklebust, Mechanism of CD79A and CD79B support for IgM+ B cell fitness through B cell receptor surface expression, J. Immunol. 209 (2022) 2042–2053.
[55] X. Agirre, J. Roman-Gomez, I. Vazquez, A. Jimenez-Velasco, L. Garate, C. Montiel-Duarte, P. Artieda, L. Cordeu, I. Lahortiga, M.J. Calasanz, et al., Abnormal methylation of the common PARK2 and PACRG promoter is associated with downregulation of gene expression in acute lymphoblastic leukemia and chronic myeloid leukemia, Int. J. Cancer 118 (2006) 1945–1953.
[56] J. Taylor, S. Wilmore, S. Marriot, K.R. Rogers-Broadway, R. Fell, A.R. Minton, T. Branch, M. Ashton-Key, M. Coldwell, F.K. Stevenson, et al., B-cell receptor signaling induces proteasomal degradation of PDCD4 via MEK1/2 and mTORC1 in malignant B cells, Cell Signal. 94 (2022) 110311.
[57] P. Juszczynski, L. Chen, E. O'Donnell, J.M. Polo, S.M. Ranuncolo, R. Dalla-Favera, A. Melnick, M.A. Shipp, BCL6 modulates tonic BCR signaling in diffuse large B-cell lymphomas by repressing the SYK phosphatase, PTPROt *Blood* 114 (2009) 5315–5321.
[58] A. Yeomans, S.M. Thirdborough, B. Valle-Argos, A. Linley, S. Krysov, M.S. Hidalgo, E. Leonard, M. Ishfaq, S.D. Wagner, A.E. Willis, et al., Engagement of the B-cell receptor of chronic lymphocytic leukemia cells drives global and MYC-specific mRNA translation, Blood 127 (2016) 449–457.
[59] D. Ribatti, F. Pezzella, Overview on the different patterns of tumor vascularization, Cells (2021) 10.
[60] C. Yang, H. Lee, S. Pal, V. Jove, J. Deng, W. Zhang, D.S. Hoon, M. Wakabayashi, S. Forman, H. Yu, B cells promote tumor progression via STAT3 regulated-angiogenesis, PLoS. One 8 (2013) e64159.
[61] M.B. Schaaf, A.D. Garg, P. Agostinis, Defining the role of the tumor vasculature in antitumor immunity and immunotherapy, Cell Death. Dis. 9 (2018) 115.
[62] Y. Qin, F. Lu, K. Lyu, A.E. Chang, Q. Li, Emerging concepts regarding pro- and anti tumor properties of B cells in tumor immunity, Front. Immunol. 13 (2022) 881427.
[63] C.M. Laumont, A.C. Banville, M. Gilardi, D.P. Hollern, B.H. Nelson, Tumour-infiltrating B cells: immunological mechanisms, clinical impact and therapeutic opportunities, Nat. Rev. Cancer 22 (2022) 414–430.
[64] J. Griss, W. Bauer, C. Wagner, M. Simon, M. Chen, K. Grabmeier-Pfistershammer, M. Maurer-Granofszky, F. Roka, T. Penz, C. Bock, et al., B cells sustain inflammation and predict response to immune checkpoint blockade in human melanoma, Nat. Commun. 10 (2019) 4186.
[65] K. Szklener, A. Michalski, K. Zak, M. Piwonski, S. Mandziuk, Ibrutinib in the treatment of solid tumors: current State of knowledge and future directions, Cells (2022) 11.
[66] S. Pal Singh, F. Dammeijer, R.W. Hendriks, Role of Bruton's tyrosine kinase in B cells and malignancies, Mol. Cancer 17 (2018) 57.
[67] W. Song, F. Fei, F. Qiao, Z. Weng, Y. Yang, B. Cao, J. Yue, J. Xu, M. Zheng, J. Li, ALKBH5-mediated N(6)-methyladenosine modification of TRERNA1 promotes DLBCL proliferation via p21 downregulation, Cell Death. Discov. 8 (2022) 25.

[68] Y. You, D. Wen, L. Zeng, J. Lu, X. Xiao, Y. Chen, H. Song, Z. Liu, ALKBH5/MAP3K8 axis regulates PD-L1+ macrophage infiltration and promotes hepatocellular carcinoma progression, Int. J. Biol. Sci. 18 (2022) 5001–5018.
[69] W. Tang, N. Xu, J. Zhou, Z. He, C. Lenahan, C. Wang, H. Ji, B. Liu, Y. Zou, H. Zeng, et al., ALKBH5 promotes PD-L1-mediated immune escape through m6A modification of ZDHHC3 in glioma, Cell Death. Discov. 8 (2022) 497.
[70] X. Qiu, S. Yang, S. Wang, J. Wu, B. Zheng, K. Wang, S. Shen, S. Jeong, Z. Li, Y. Zhu, et al., M(6)A demethylase ALKBH5 regulates PD-L1 expression and tumor immunoenvironment in intrahepatic cholangiocarcinoma, Cancer Res. 81 (2021) 4778–4793.
[71] C. Wei, B. Wang, D. Peng, X. Zhang, Z. Li, L. Luo, Y. He, H. Liang, X. Du, S. Li, et al., Pan-cancer analysis shows that ALKBH5 is a potential prognostic and immunotherapeutic biomarker for multiple cancer types including Gliomas, Front. Immunol. 13 (2022) 849592.
[72] S. Kumar, T. Mohapatra, Deciphering epitranscriptome: modification of mRNA bases provides a new perspective for post-transcriptional regulation of gene expression, Front. Cell Dev. Biol. 9 (2021) 628415.
[73] I. Lopez de Silanes, J. Fan, C.J. Galban, R.G. Spencer, K.G. Becker, M. Gorospe, Global analysis of HuR-regulated gene expression in colon cancer systems of reducing complexity, Gene Expr. 12 (2004) 49–59.
[74] J.H. Lumb, Q. Li, L.M. Popov, S. Ding, M.T. Keith, B.D. Merrill, H.B. Greenberg, J. B. Li, J.E. Carette, DDX6 Represses aberrant activation of interferon-stimulated genes, Cell Rep. 20 (2017) 819–831.
[75] F. Yang, T. Bian, X. Zhan, Z. Chen, Z. Xing, N.A. Larsen, X. Zhang, Y. Shi, Mechanisms of the RNA helicases DDX42 and DDX46 in human U2 snRNP assembly, Nat. Commun. 14 (2023) 897.
[76] R. Hirabayashi, S. Hozumi, S. Higashijima, Y. Kikuchi, Ddx46 is required for multi-lineage differentiation of hematopoietic stem cells in Zebrafish, Stem Cells Dev. 22 (2013) 2532–2542.
[77] L. Chen, M. Xu, W. Zhong, Y. Hu, G. Wang, Knockdown of DDX46 suppresses the proliferation and invasion of gastric cancer through inactivating Akt/GSK-3beta/beta-catenin pathway, Exp. Cell Res. 399 (2021) 112448.
[78] Z. Ma, J. Song, Y. Hua, Y. Wang, W. Cao, H. Wang, L. Hou, The role of DDX46 in breast cancer proliferation and invasiveness: a potential therapeutic target, Cell Biol. Int. 47 (2023) 283–291.
[79] H. Wu, Y. Hu, X. Liu, W. Song, P. Gong, K. Zhang, Z. Chen, M. Zhou, X. Shen, Y. Qian, et al., LncRNA TRERNA1 function as an enhancer of SNAI1 promotes gastric cancer metastasis by regulating epithelial-mesenchymal transition, Mol. Ther. Nucleic. Acids. 8 (2017) 291–299.
[80] W. Wang, X. Tang, H. Qu, Q. He, Translation regulatory long non-coding RNA 1 represents a potential prognostic biomarker for colorectal cancer, Oncol. Lett. 19 (2020) 4077–4087.
[81] Y. Qian, Y. Li, Y. Ge, W. Song, H. Fan, Elevated LncRNA TRERNA1 correlated with activation of HIF-1alpha predicts poor prognosis in hepatocellular carcinoma, Pathol. Res. Pract. 227 (2021) 153612.
[82] X. Wang, Y. Ren, X. Yang, X. Xiong, S. Han, Y. Ge, W. Pan, L. Zhou, Q. Yuan, M. Yang, miR-190a inhibits epithelial-mesenchymal transition of hepatoma cells via targeting the long non-coding RNA treRNA, FEBS Lett. 589 (2015) 4079–4087.
[83] W. Song, Y. Gu, S. Lu, H. Wu, Z. Cheng, J. Hu, Y. Qian, Y. Zheng, H. Fan, LncRNA TRERNA1 facilitates hepatocellular carcinoma metastasis by dimethylating H3K9 in the CDH1 promoter region via the recruitment of the EHMT2/SNAI1 complex, Cell Prolif. 52 (2019) e12621.
[84] Y. Cheng, Y. Fu, Y. Wang, J. Wang, The m6A methyltransferase METTL3 is functionally implicated in DLBCL development by regulating m6A modification in PEDF, Front. Genet. 11 (2020) 955.
[85] S. Mukhopadhyay, M.E. Amodeo, A.S.Y. Lee, eIF3d controls the persistent integrated stress response, Mol. Cell 83 (2023) 3303–3313, e3306.
[86] F. Yu, J. Wei, X. Cui, C. Yu, W. Ni, J. Bungert, L. Wu, C. He, Z. Qian, Post-translational modification of RNA m6A demethylase ALKBH5 regulates ROS-induced DNA damage response, Nucleic. Acids. Res. 49 (2021) 5779–5797.
[87] P. Wang, J. Wang, S. Yao, M. Cui, Y. Cheng, W. Liu, Z. Gao, J. Hu, J. Zhang, H. Zhang, Deubiquitinase USP9X stabilizes RNA m(6)A demethylase ALKBH5 and promotes acute myeloid leukemia cell survival, J. Biol. Chem. 299 (2023) 105055.
[88] X.L. Zhang, X.H. Chen, B. Xu, M. Chen, S. Zhu, N. Meng, J.Z. Wang, H. Zhu, D. Chen, J.B. Liu, et al., K235 acetylation couples with PSPC1 to regulate the m(6)A demethylation activity of ALKBH5 and tumorigenesis, Nat. Commun. 14 (2023) 3815.